INTER/47-15-6

INTER

International Network on Timber Engineering Research

AN ELASTOPLASTIC SOLUTION FOR EARTHQUAKE RESISTANT RIGID TIMBER SHEAR WALLS

Wei Yuen Loo
P Quenneville
N Chouw

Department of Civil and Environmental Engineering
The University of Auckland

NEW ZEALAND

BATH
UNITED KINGDOM
SEPTEMBER 2014

An elastoplastic solution for earthquake resistant rigid timber shear walls

Wei Yuen Loo, Pierre Quenneville, Nawawi Chouw

Department of Civil and Environmental Engineering, the University of Auckland

Auckland, New Zealand

Keywords: Shear walls, elasto-plastic, slip-friction connectors, energy-dissipation, ductility.

1 Introduction

In terms of seismic performance, timber structures have been observed to perform well, in spite of timber being an inherently non-ductile material. This is due mainly to the ductility of the steel-to-timber connections, and the way in which they interact with the timber material. If these connections are detailed to deform plastically, while keeping the timber members elastic, the overall structure achieves ductility. For nailed sheathing-to-framing shear walls and floor diaphragms, the New Zealand structural timber code, NZS3603:1993 [1] allows ductilities of up to four to be assumed. The issue with such an approach is that in a design level earthquake, the deformations required to achieve ductility often renders the structure irreparable, or at least requiring expensive repairs. Recent developments in engineered lumber products have seen the availability of mass timber panels of tremendous strength and stiffness. These include CLT (cross laminated timber) and LVL (laminated veneer lumber) panels. Under typical loading conditions these panels are essentially rigid, and the experiments of Popovski and Karacabeyli [2] demonstrate that the hysteretic behaviour is largely governed by the plastic deformations in the steel bracket connections attaching the walls to the floor. The hysteretic loops bear some resemblance to those of sheathing to framing shear walls, the main difference being they are more tightly pinched. The seismic performance of such walls is adequate, however, damage is still a consequence after an earthquake.

The authors propose implementing energy dissipating slip-friction device as hold-down connectors in shear walls (see Fig. 1(a)). By adjusting the slip-force of the connectors, the strength of the wall can be tuned to a desired strength, and overturning moment (and hence activated base shear) capped below a certain threshold. Because the force-displacement behaviour of the connectors is highly elasto-plastic (see Fig. 1(b)), it is expected that this characteristic would be reflected in the hysteretic behaviour of the walls in which they serve as hold-downs. Numerical modeling has demonstrated the promise of such a concept [3].

This paper introduces experiments carried out on a 2.4 m × 2.4 m LVL wall with slip-friction connectors. To facilitate controlled rocking, a novel shear key is adopted, that contributes to the damping of the system. The respective contributions to wall strength of the shear key and the slip-friction device can be quantified by a simple analytical relationship, and the predicted results align closely with the experimental results.

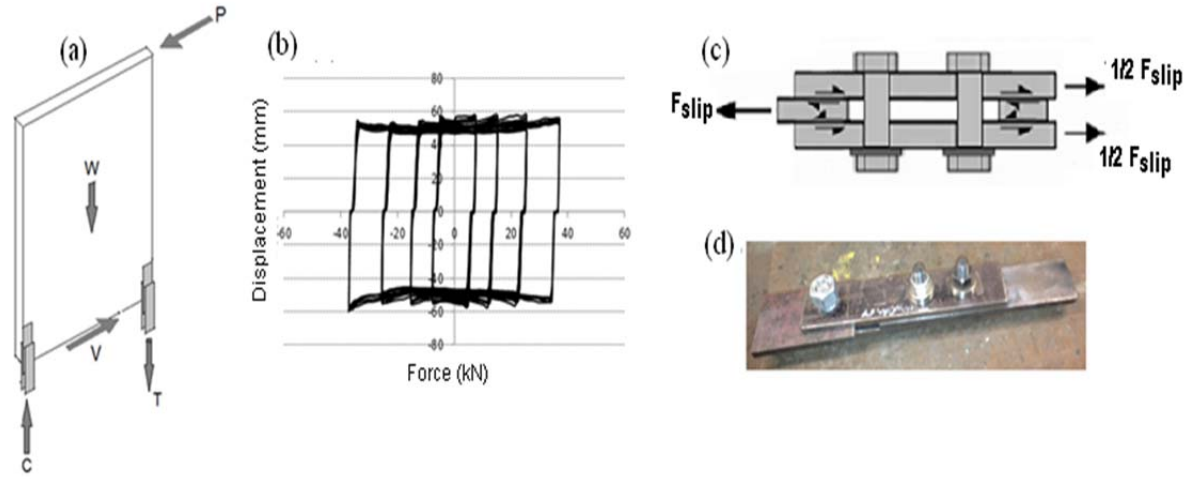

Figure 1 (a) General concept (frictional effects from shear key not shown), (b) hysteretic behaviour of slip-friction connector from component test, (c) forces on connector, and (d) connector specimen.

Implications to the way in which such a system could be designed, and considerations unique to them are discussed. The modelling of the wall and connectors is covered, and earthquake simulations are used to investigate the seismic performance of the wall. The results are presented and discussed.

2 Slip-friction connectors

The type of slip-friction connector (see Figure 1(d)) adopted as wall hold-downs has a symmetric sliding mechanism, in which the two outside plates resist in equal proportion the external load applied to the centre-plate (see Fig. 1(c)). Other researchers have used slip-friction connectors in steel frames [4] - however those typically have an asymmetric mechanism, in which external load is only applied to the centre plate, and one of the outside plates. Butterworth [5] provides a detailed discussion of the sliding mechanism of both symmetric and asymmetric connectors. Symmetric connectors were explored in great detail by Popov and Grigorian [6], and to date, these have typically required the use of brass shims between mild steel surfaces in order to facilitate sliding. Without brass shims, it has been shown that sliding is extremely erratic. However, in the connector design for the shear wall, the authors decided to forgo the use of shims altogether, and instead simply use a centre-plate of abrasion resistant steel (typically Bisalloy 400), in direct sliding against external mild steel plates. All steel surfaces were prepared to the clean mill scale finish prior to use, and extensive tests carried out by Loo et al. [7] show that with some minor preconditioning of the surfaces, while keeping the connectors clamped together, excellent elasto-plastic behaviour can be achieved (see Fig. 1(b)).

3 Experimental wall with slip-friction connectors

A 2.44 m × 2.44 m wall was assembled from two separate 1.22 m × 2.44 m LVL panels of 45 mm in thickness (see Fig. 2(a)). Loo et al. [8] describes the set-up of the experimental wall; the panels were fabricated through the use of screws connecting the panels through end studs, and top and bottom plates. These plates were fabricated from the same material as the main wall. In the design, a maximum racking force of approximately 120 kN was considered (the actual maximum tested force was between 65 and 70 kN).

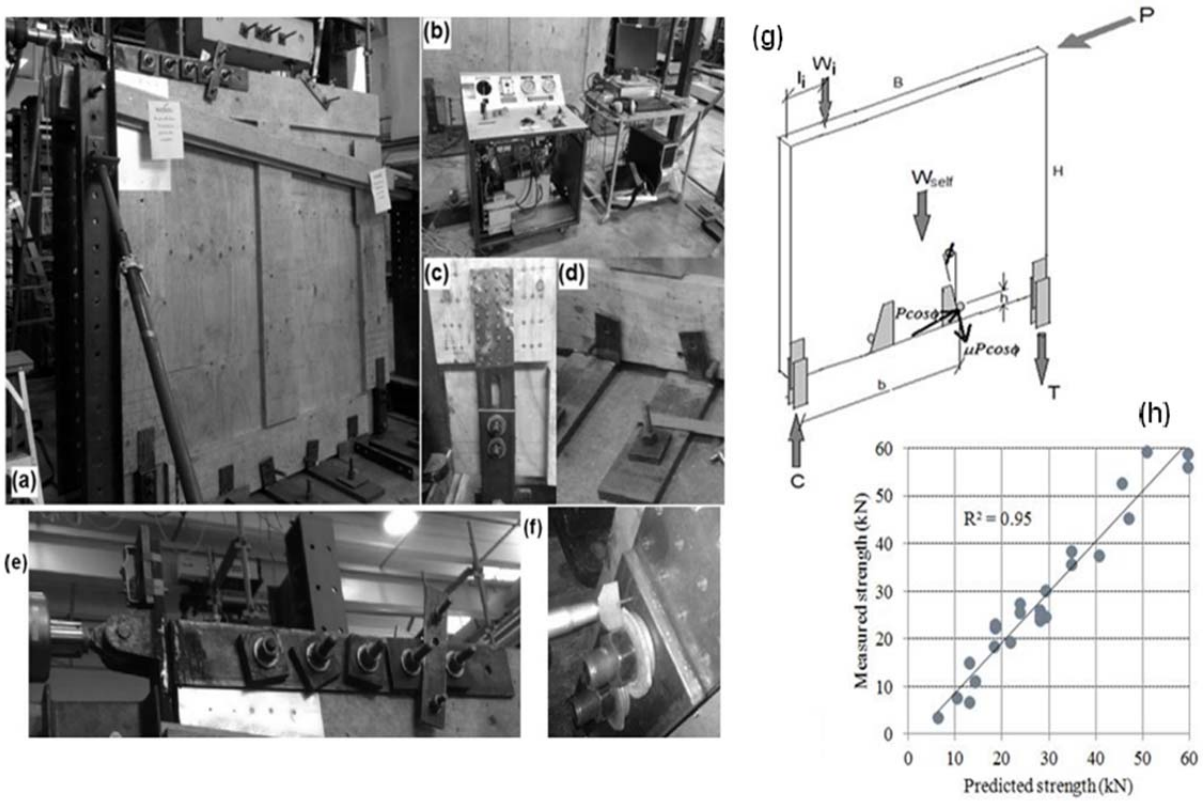

Figure 2 (a) General setup, (b) actuator controller and data acquisition system, (c) slip-friction connector shown extended, (d) shear key, (e) plates to transfer racking force, and (f) use of depth micrometre to measure deflection of Belleville washer stack. (g) Forces on wall about to uplift, with racking force P applied at the top corner. (h) Measured strength vs. predicted strength.

A slip-friction connector riveted to an end chord is shown in Fig. 2(c), and the shear key of two vertical steel plates and solid steel rod inserts is shown in Fig. 2(d). Because the wall in itself is almost rigid and the actual material yield strength would be well beyond the range of the test values, its strength is controlled by the slip-friction connectors. Belleville washers were again employed to provide the desired preload. This preload in the bolts is a function of the way the Belleville washers are stacked in parallel and series, and the deflection applied to the stack. Loo et al. [8] derived expressions to find the Belleville stack height for a desired slip-force. A depth micrometre was used to gauge the deflection of the Belleville washers (see Fig. 2(f)). When the slip-force of the connector is achieved, the wall will uplift and rock. In order for rocking to occur in a relatively unimpeded manner, a shear key is proposed in which solid steel rods passing through the timber panel are made to bear on mild steel shear plates on both sides of the wall. These plates are rigidly fixed to the foundation, and the bearing surface is set at a slight angle from the vertical.

The free body diagram of the wall just about to uplift is shown in Fig. 2(g), and the expression for racking force is:

$$\mathbf{P} = \frac{\mathbf{F_{slip}B} + \frac{\mathbf{W_{self}B}}{2} + \sum_{\mathbf{i=1}}^{\mathbf{n}} \mathbf{W_i l_i}}{\mathbf{H - K_{mrp}}} \tag{1}$$

where K_{mrp} encapsulates the effect and contribution of the shear key:

$$K_{mrp} = (h^2 + b^2)^{1/2} \cos \emptyset \left[\mu \cos\left(\emptyset - \tan^{-1}\left(\frac{h}{b}\right)\right) - \sin\left(\emptyset - \tan^{-1}\left(\frac{h}{b}\right)\right)\right] \quad (2)$$

Loo et al. [8] describes 25 tests carried out on the wall, with the experimentally measured strengths corresponding well with the values from Eq. 1 (see Fig. 2(h)). No damage to the wall was observed. The connectors each underwent at least 14 m of cumulative sliding travel, with little evidence of deterioration in strength or stiffness. Fig. 3(a) shows a typical hysteretic result, and Fig. 3(b) shows the uplift displacement time history at the slip-friction connector locations. One end of the wall readily descends, while the other end uplifts. This capability to re-centre under only self-weight (approximately 2.8 kN), demonstrates the accuracy obtained in setting the connector force (the difference in the slip-force between connectors is required to be less than the combined gravity effects [8] for re-centring to take place), and this capability is naturally an important prerequisite for minimising residual drifts following an earthquake.

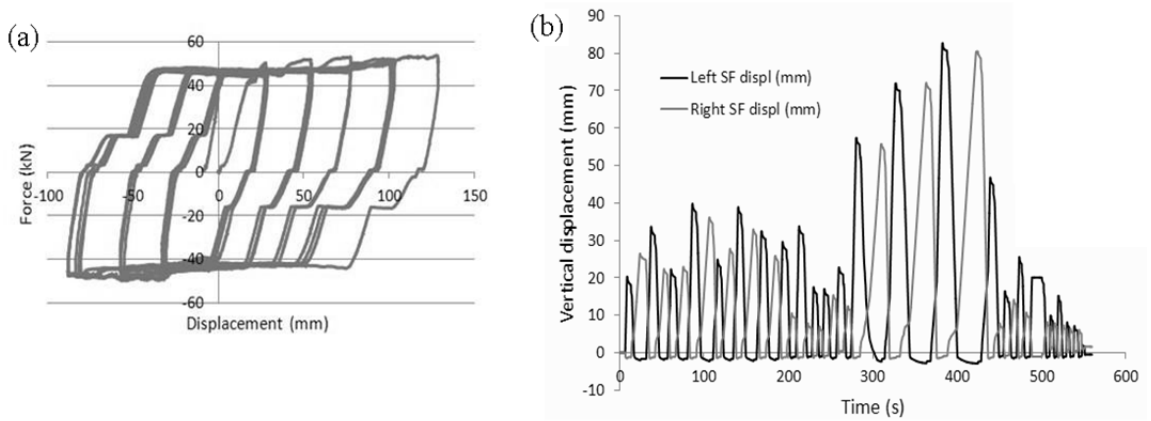

Figure 3 (a) Force-displacement behaviour for wall of approximate 45 kN strength. (b) Vertical displacement time history at slip-friction connector locations.

The reader is referred to Loo et al. [8] for a detailed presentation and analysis of the experimental results.

4 General design imperatives

4.1 Ductility

Slip-friction connectors applied to rigid walls can readily enable elasto-plastic behaviour. The amount of ductility is limited only by the length of travel allowed by the slot within the centre-plate of the connector. Such a slot should provide enough sliding distance to correspond to little or no damage during a design level earthquake, and even perhaps a maximum credible earthquake. In extreme circumstances, this drift could be exceeded, and the priority under such a circumstance is to shift the ductility demand to the other steel connections within the structure, ensuring the structure maintains strength and avoids brittle damage.

For timber structures, definitions of yield strength and ductility have varied [9]. Yield strength can be somewhat difficult to define, because in reality the load-slip relationship of timber connections is not strictly linear at any portion of the load-slip envelope. Nevertheless, 50% of ultimate strength has been commonly used in the past for sheathing to framing shear walls. For CLT walls, strengths are currently defined as 40% that of the ultimate strength [10]. The overall ductility μ is found by dividing the failure displacement,

δ_{max}, (typically the displacement at which the strength falls to 80% of the peak load) by the yield displacement δ_y. These definitions are illustrated in Fig. 4(a). For walls with slip-friction connectors, the same approach can be adopted to define overall ductility, μ. Fig. 4(b) shows that within the overall ductility, such walls enjoy a damage free phase, as well as a quite distinct region involving inelastic damage. The damage free zone is associated with the slip-friction connectors undergoing sliding, and thereby capping forces at or below the yield strength of the wall (i.e 50% of ultimate load for sheathing to framing walls, and 40% of ultimate load for CLT walls). The measure of slip-friction enabled ductility is $\mu_{sf} = \delta_{sf} / \delta_y$. It is intended that during earthquakes the structures remains in the damage free zone with a high level of probability.

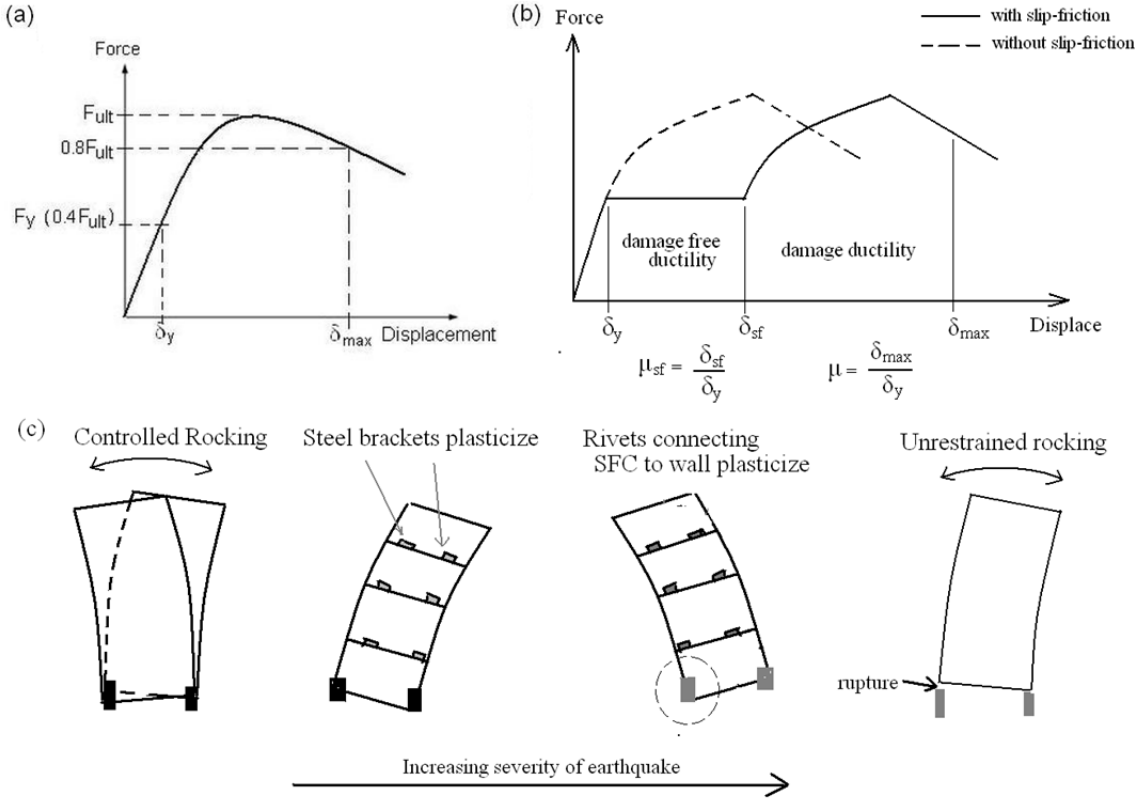

Figure 4 (a) Definitions of wall strength and maximum displacement. (b) Total and slip-friction enabled ductility for wall with slip-friction connectors, and (c) a possible progression of nonlinearity for CLT wall structure.

The designer would decide on an appropriate value for δ_{sf}, corresponding to relevant code recommendations of drift for a ULS or MCE event. It is emphasised that the continued ductile behaviour of the wall beyond δ_{sf} (second phase ductility), depends on sufficient overstrength being provided when designing the other connections of the structure. For sheathing-to-framing walls, this second phase ductility would be supplied by the deformation of the nail connections, while for CLT walls, it would arise from the the ductil plasticization of the steel bracket connections.

Within the structure, sources of ductility are the slip-friction connector, and the steel brackets at each storey connecting the wall to the floor below. The rivets connecting the slip-friction connector to the wall should be designed for a ductile failure mode. A possible order of 'non-linearization' is illustrated in Fig. 4(c).

Naturally the first stage involves sliding of the slip-friction connectors and uplift and rocking of the wall. It is intended that for almost all design level events, and for most maximum credible events, the non-linear behaviour of the wall structure will remain in this

range. However an extreme event could cause the wall to attempt to uplift past the range permitted by the connector slot-lengths. A second phase of nonlinear behaviour is then intiated (the post-plateau part of Fig. 4(b)). During this phase, ductility is achieved through the plasticization of the steel brackets, and some rocking of the non-ground floor wall panels – in fact this is the mechanism currently depended upon to provide adequate seismic performance [2]. But whereupon in current practice, the ductile behaviour of the steel brackets constitutes the first stage of ductility, in the proposed concept it will serve as reserve ductility only.

If for some reason ductility in the inter-storey steel bracket connections is not manifested in the manner desired, or the event is so extreme as to cause extremely large displcements, the third stage of non-linearity is provided by the riveted connection between the slip-friction connector and the timber wall (note that the assumption is that it is preferable to have damage first occur in the steel bracket connectors, rather than risk the rupturing away of the slip-friction connector from the wall). The slip-friction connector should be designed for a ductile mode of failure, and this is readily achieved through reference to the work of Zarnani and Quenneville [11, 12]. Upon the complete loss of strength in the riveted connection, the wall will freely rock.

It should be emphasised that the final stage may superficially appear to mean collapse, but this is not necessarily the case. In fact something akin to free rocking is already assumed as providing adequate behaviour in current design practice of CLT walls [10]. Regardless of the intensity of an earthquake event, brittle failure of the timber members should be avoided. Thus it is also necessary to check that the actions associated with the overstrength levels of all the connectors, will not cause any of the timber members to exceed their respective yield strengths.

4.2 Rocking and shear amplification

In the case of MDOF structures designed to rock, numerical studies have shown that higher mode effects can play a part in increasing the shear action above those predicted by the equivalent static method (which is based on the fundamental mode of vibration). Kelly [13] carried out a series of numerical analyses, and from this proposes the following dynamic amplification factor, ω_v, to be used to increase the shear actions.

$$\omega_v = 1 + a_{VN}DF \quad \text{for } N > 1 \tag{3}$$

where DF is the ductility and a_{vn} is a shear amplification factor with values of 0, 0.1, 0.15, 0.40, 0.60, and 0.90 for 1, 2, 3, 4, 5, and 6 story buildings, respectively. A detailed discussion of this factor and its development is provided by Kelly [13]. The authors adopt Eq. 3 in the discussion of earthquake simulation results in Section 6.

5 Numerical model

5.1 Multi-storey wall

In order to demonstrate the benefits of slip-friction connectors, a five storey shear wall is designed, modelled, and placed under earthquake simulations. The software package SAP2000 [14] was used. The model wall is considered to be one of the perimeter walls of a 6 m × 6 m box structure. It is assumed that only the perimeter walls resist earthquake forces. Storey heights are 2.6 m, and the concentrated seismic mass at all levels is 15

tonnes. Walls are of 140 mm thick CLT panels at every storey, and are modelled by a thick shell element. The shell elements have an elastic modulus of 10200 MPa, and shear modulus of 525 MPa. In terms of gravity, only self-weight is considered. The wall was designed for the seismically active area of Napier, New Zealand, and intermediate soil type conditions. The design ductility is 4, and the fundamental period found to be approximately 0.7 s. Based on the spectral acceleration and procedure of NZS 1170.5:2004 [15], the lateral forces F_i at each level are calculated. These are presented in Table 1, together with the shear and bending actions.

Table 1 Distributed forces and actions on shear wall

Floor	h (m)	m (kg)	$m_i h_i$	$m_i h_i$ /sum($m_i h_i$)	F_i (kN)	V (kN)	M (kNm)
5	13	15000	195000	0.33	27.0	27.0	0.0
4	10.4	15000	156000	0.27	17.1	44.2	70.3
3	7.8	15000	117000	0.20	12.9	57.0	185.1
2	5.2	15000	78000	0.13	8.6	65.6	333.4
1	2.6	15000	39000	0.07	4.3	69.9	504.0
0	0		585000			69.9	685.7

5.2 Connections

5.2.1 Steel brackets

Steel bracket connections were adopted in connecting the walls to the floor panels below. For simplicity of modelling, the same bracket type was used, with the required overturning resistance obtained by varying the distribution of the brackets. The assumed mechanism of the rocking wall with plasticizing bracket connections is shown in Fig. 5(a).

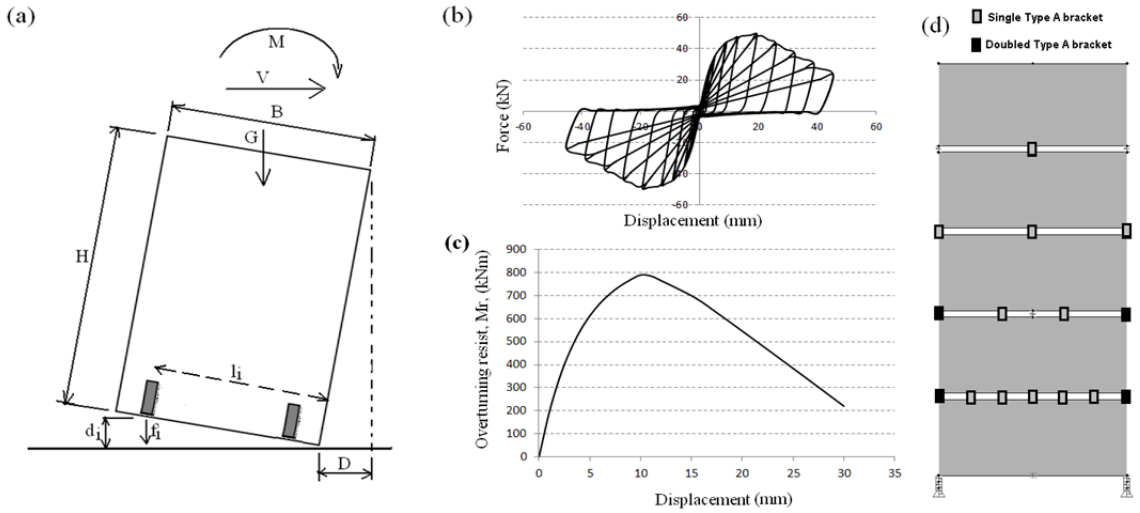

Figure 5(a) Free body diagram of shear wall panel, adapted from [10] (b) Numerical hysteretic behaviour of Type A bracket. (c) Resistance to overturning as a function of displacement, D, for a 2.6 m high by 6 m wide wall with doubled Type A brackets at the ends and singles at l_i = 2 m and 4 m. (d) Distribution of brackets in model wall.

If the wall had *n* brackets, the overturning resistance M_r is

$$M_r(D) = \sum_{i=1}^{n} l_i f_i \langle \frac{l_i}{H} D \rangle + \frac{L}{2} G \quad (4)$$

Note that f_i is a function of (l_i D / h). To resist a design level overturning action (peak value divided by 2.5), brackets must be designed and laid out in such a way so that

$$M_r \geq V\,H + M \tag{5}$$

The bracket adopted for modelling is reported on by Shen et al. [16]. Averaged hysteretic parameters from cylic tests on a SIMPSON strong tie steel 90×48×3×116 mm bracket with eighteen 3.8 × 89 mm spiral nails (conveniently called bracket Type A) are provided by Shen et al., and these are reproduced in Table 2. Adopting these parameters and using a multilinear plastic link, the method of Loo et al. [17] was used to model the force-displacement behaviour of Type A brackets. This method is largely based on the behaviour on the well known Foschi load-slip curve for steel connections in timber structures.

A result from a numerical test on a single Type A bracket is shown in Fig. 5(b). Fig. 5(c) shows the moment-resistance / racking-displacement relationship (from Eq. 4) for a 6 m wide by 2.6 m high wall, with single connectors at l_i = 2 m and 4 m, and doubled connectors at the ends. For the model wall, the connection arrangements for each wall panel are shown in Fig. 5(d) (note that the distributions do not necessarily reflect a practical implementation, but serve to investigate the adopted design principles and how they perform under simulation).

5.2.3 Slip-friction connector

The slip-friction connector is modelled using a gap, hook, and multilinear plastic element. The gap element prevents the downward displacement of the wall at its corner, the hook element defines the slot-length available for sliding (i.e. uplift), and the multilinear plastic link with kinematic hysteris behaviour provides the elasto-plastic characteristics of the connector. Loo et al. [3] describes in detail the modelling of slip-friction connectors. In the research of this article, the slip-friction connector is placed in series with the element representing the rivet connection to the wall (see Fig. 6(a)).

The sliding strength, F_{slip}, of the slip-friction connector is set as:

$$F_{slip} = \frac{M_o}{B} - \frac{G}{2} \tag{6}$$

where M_o is the overturning moment on the wall, and G the total gravity effects including self-weight. M_o for the model wall is 686 kNm (see Table 1) and G (assuming self-weight only, and 450 kg/m^3 for CLT) is 48.2 kN. Thus, F_{slip} is set to 90 kN. The slot length was set for a maximum allowable uplift of 150 mm, i.e corresponding to 2.5% drift.

5.2.4 Rivet connections

Timber rivets provide an excellent solution in timber structures, where both a stiff connection and high force to transfer area ratio, is required. This suits the requirements of the connection between the slip-friction connector and shear wall (see Fig. 2(c)). In general, riveted connections should be designed for a ductile failure mode, and brittle failure modes such as block pull-out and splitting should be avoided. Zarnani and Quenneville [11, 12] investigated rivets in timber and provide design equations enabling their ductile design. Popovski and Karacabeyli [18] tested rivets on braced frames and obtained averaged force-displacement properties for various timber types such as glulam, parallel strand lumber, and laminated veneer lumber (LVL). Zarnani and Quenneville have investigated CLT - however these are yet to be published. Thus the values for laminated

veneer lumber are adopted for modelling purposes, and presented in Table 2. For comparison, results for a nail connection are also shown.

Table 2 Averaged Foschi parameters for single rivet, nail, and bracket Type A

Foschi parameter	[1]Rivet (40 mm long)	[2]Nail (3 mm dia)	[3]Bracket Type A (18 spiral nails)
Ultimate strength, F_{ult} (kN)	3.2	1.37	49.1
Displacement at ultimate strength, δ_{ult} (mm)	3.3	9	20
Strength at failure (80% of F_{ult}), F_{fail} (kN)	2.6	1.1	39.2
Displacement at failure, δ_{fail} (mm)	7.7	14.9	29.4
Initial stiffness, K_0 (kN/mm)	3.8	1.2	11.93
Tangent stiffness at peak load, K_1 (kN/mm)	0.41	0.05	0.012
Post peak strength envelope gradient, K_2 (kN/mm)	-0.15	-0.042	-1.05
Unloading stiffness, K_3 (kN/mm)	3.6	1.1	11.3
Pinching strength, F_1 (kN)	0.27	0.19	4
Y-intercept strengthe, F_0 (kN/mm)	1.9	0.92	49.27

[1]adopted (or estimated by authors) from Popovski and Karacabeyli [18]

[2] adopted (or estimated by authors) from Dolan and Madsen [19]

[3] adopted (or estimated by authors) from Shen et al. [16]

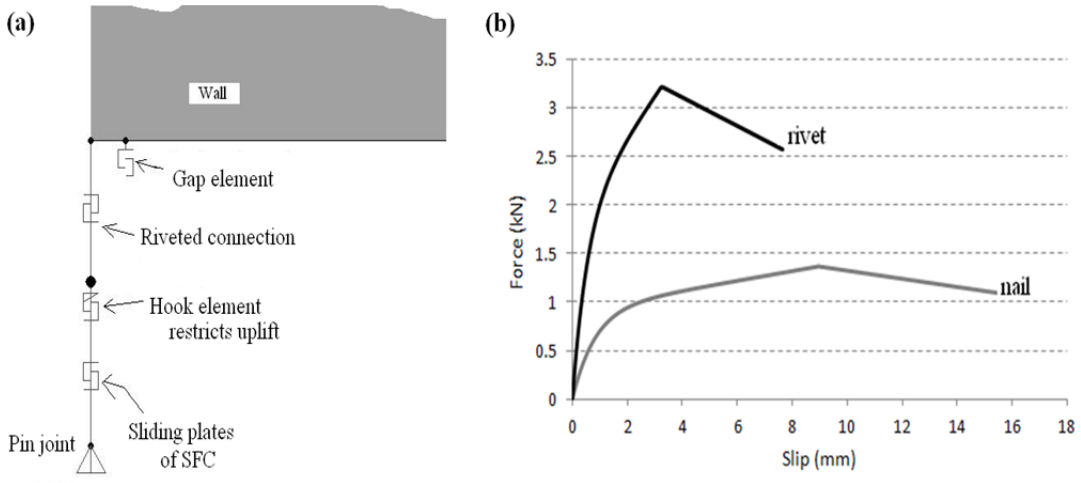

Figure 6 (a) Riveted connection combined with slip-friction elements. (b) Foschi load-slip curves for a timber rivet, compared with a 3 mm diameter nail.

The Foschi envelope curve for the rivet is compared to that of the 3 mm diameter nail in Fig. 6(b), and the differences in strength and stiffness are apparent. While rivets do exhibit high levels of ductility (around 15 for LVL), only a very small displacement post-peak load will cause failure, and this is an important consideration when it comes to providing post-sliding ductility to the structure (see Fig. 4(c)). Rivet connections are modelled using a multilinear plastic element of a pivot hysteresis type. Note that a connection with *n* rivets has *n* times the strength and stiffness values of Table 2 (the assumption being that significant displacements remain the same [17]). Fig. 6(a) shows the element representing the rivet as part of the overall slip-friction connector.

6 Earthquake simulations – results and discussion

The wall was subjected to five earthquake simulations. The acceleration records and their respective scale factors are shown below.

Table 3 Earthquake acceleration records[a]

Event	Station	Bearing	PGA (g)	Scale Factor, k_1[b]	Scaled PGA (g)
El Centro, Imperial Valley, 1940	117 El Centro Array #9	180°	0.313	0.9	0.282
Loma Prieta 1989	47125 Capitola	0°	0.529	0.6	0.317
Northridge 1994	24303 LA – Hollywood Stor	90°	0.231	1.5	0.347
Kobe 1995	0 JMA	0°	0.821	0.3	0.246
Chihuahua 1979	6621 Chihuahua	282°	0.254	0.9	0.229

[a]From PEER [20]

[b]Scaled for building period of 0.7 s. Location Napier, NZ, 500 yr return period, Site C soils.

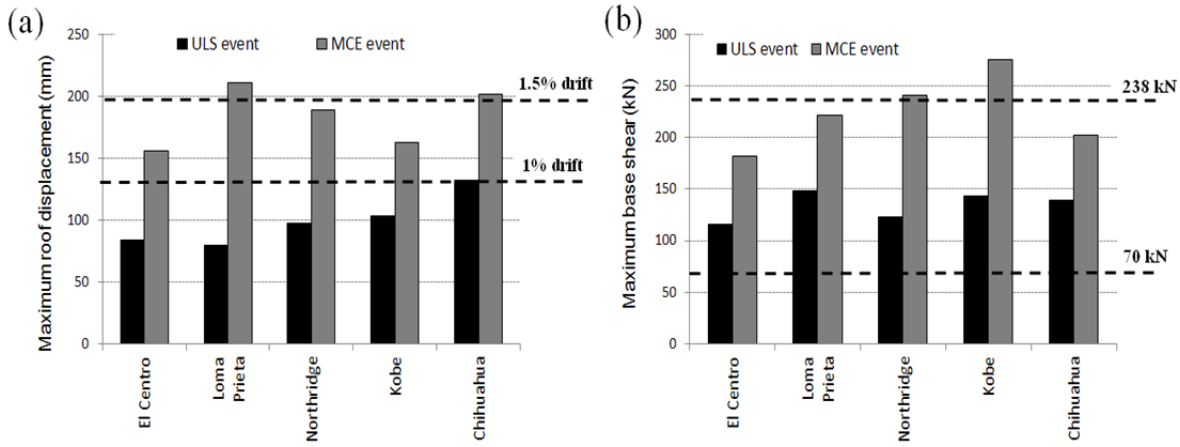

Figure 7 (a) Maximum displacements, and (b) maximum base shears

From Fig. 7(a) it can be seen that the maximum roof displacements are generally below a 1% drift limit, while drifts for two of the MCE event are slightly above 1.5%. From a performance based approach this is promising, as the NZS1170.5 [15] limit for the ULS state allows 2.5%. It should be noted that residual drifts are not shown. This is because in all cases, both the ULS and MCE residual drifts were close to, if not zero, and all well below the 0.2% limit for realistic self-centring structures [21].

Base shears are shown in Fig. 7(b). It is seen that the equivalent static predicted value of 70 kN is significantly exceeded in both the ULS and MCE events. This is due to higher mode effects on the structure that amplifying the base shears initiating uplift. From Eq. 3, the dynamic amplification factor is $\omega_v = 3.4$ for a 5 storey structure, and this gives a value of 238 kN. Fig. 7(b) shows this value as conservative for the ULS case, but appropriate to the MCE case.

In the modelling of the wall, the brackets, slip-friction connectors, and the rivets connecting the slip-friction connector to the wall were designed for the same level of

actions, with no overstrength between them. However, in Fig. 4(c), a possible progression of nonlinearity was presented. In order to explore the impact of a 'weak' rivet connection and a 'strong' bracket connection, the model is adjusted, and the slot length reduced to 50 mm (from the original 150 mm), in order to allow the second phase of ductile behaviour shown in Fig. 4(b) to develop. The El Centro MCE simulation was applied, and the hysteretic result from one of the rivet connections is shown in Fig. 8(a). Clearly the rivet connection (attaching the slip-friction connector to the wall) is more or less behaving elastically, and has undergone little damage, in spite of the reduction in slot length.

With the same slot length of 50 mm retained –the strength and stiffness of the Type A brackets within the wall were then increased by 1.5.

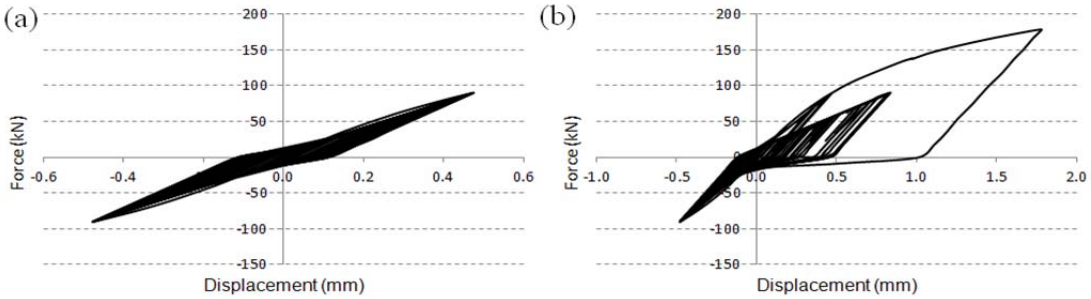

Figure 8 Hysteresis of rivets when (a) wall is not overstrengthened, and (b) when wall is overstrengthened. Note the difference in scale of the horizontal axis.

The impact on the same rivet connection is startling, and Fig 8(b) shows evidence of significant non-linear damage. With further excitations, failure of this connection is highly likely. Clearly, careful consideration should be given, when overstrengthening the nonlinearly responding parts of the structure relative to one another.

7 Conclusions

Experimental work on a rocking wall with slip-friction connectors demonstrate the feasibility of the concept, and the wall manifests excellent elasto-plastic behaviour and readily rocks back into place as long as the connector strengths are within a range no larger than the gravity loads on the wall. That this occurs under just self-weight indicates that the method of directly measuring Belleville washer displacement in order to modulate the slip-force in the connectors can be achieved with reasonable precision.

Slip-friction connectors allow available ductility to be directly determined through the provision of slot lengths corresponding to particular target rotational drift levels. Two measures of ductility can thus be defined. Slip-friction enabled ductility represents a damage free zone of ductile behaviour, while total ductility (failure displacement divided by yield displacement) includes both this damage free range and also a zone where plasticization of the brackets connecting the walls to the floor below occurs.

Slip-friction connectors thus have the potential to enhance the already adequate seismic performance of CLT walls, by allowing the wall to avoid damage for a large range of drift, but with a backup reservoir of ductility provided through the ductile bracket connections connecting each wall panel to the storey directly below it, as is currently the case. However care must be taken to avoid premature failure of the very stiff rivet connection. This can be

done by ensuring the riveted connection is designed for actions that are the same, or preferably higher than those of the brackets.

Numerical parametric studies are currently being conducted to determine the ranges of uplift that correspond to design level and maximum credible earthquakes within and their probabilities of non-exceedance.

References

[1] Timber structures standard, NZS3603, Standards New Zealand, Wellington, New Zealand; 1993.

[2] Popovski M, Karacabeyli E. Seismic behaviour of cross-laminated timber structures. Auckland, New Zealand: Proc of World Conference on Timber Engineering; 2012.

[3] Loo WY, Quenneville P, Chouw N. A numerical study of the seismic behaviour of timber shear walls with slip-friction connectors. Eng Struct 2012; 34(22):233-243.

[4] Khoo HH, Clifton GC, Butterworth JW, MacRae G, Ferguson G. Influence of steel shim hardness on the Sliding Hinge Joint performance. J Constr Steel Res 2012; 72(2012):119-129.

[5] Butterworth J. Ductile concentrically braced frames using slotted bolted joints. J Struct Eng Society of New Zealand 2000; 13(1):39–48.

[6] Popov E, Grigorian C, Yang T. Developments in seismic structural analysis and design. Eng Struct 1995; 17(3):187–97.

[7] Loo WY, Quenneville P, Chouw N. A new type of symmetric slip-friction connector. J Constr Steel Res; 94(March 2014): 11-22.

[8] Loo WY, Kun C, Quenneville P., Chouw N. Experimental testing of a rocking timber shear wall with slip-friction connectors. Earthq Eng Struct D 2014; DOI: 10.1002/eqe.2413

[9] Munoz W, Salenikovich A, Mohammad M, Quenneville P. Determination of yield point and ductility of timber assemblies: in search for a harmonised approach. In: Proceedings of Meeting 41 of CIB-W18, St Andrews, Canada; 2008

[10] Gagnon S, Pirvu C. CLT Handbook: Cross-Laminated Timber. FPInnovations, Canada, 2011.

[11] Zarnani P, and Quenneville P. Strength of timber connections under potential failure modes - An improved design procedure. Constr Build Mater, 60(June 2014): 81-90.

[12] Zarnani P, and Quenneville P. Wood block tear-out resistance and failure modes of timber rivet connections – a stiffness-based approach. J Struct Eng 2014; 140(2), 04013055.

[13] Kelly TE. Tentative seismic design guidelines for rocking structures. B NZ Soc for Earthq Eng 2009; 42(4):239-274.

[14] Computers and Structures, Inc. SAP2000 v14: Integrated solution for structural analysis and design. Berkeley, California; 2009.

[15] Structural design actions - Part 5: Earthquake actions, NZS1170.5, Standards New Zealand, Wellington, New Zealand; 2004.

[16] Shen Y-L, Schneider J, Tesfamariam S, Steimer S, Mu Z-G. Hysteresis behavior of bracket connection in cross-laminated-timber shear walls. Eng. Struct; 48(November 2013): 980-991.

17] Loo WY, Quenneville P, Chouw N. A numerical approach for simulating the behaviour of timber shear walls, Struct Eng Mech 2012; 42(3): 383-407.

[18] Popovski M, Karacabeyli E. Seismic performance of riveted connections in heavy timber construction. Vancouver, Canada: 13th World Conference on Earthquake Engineering; 2004.

[19] Dolan JD and Madsen B. Monotonic and cyclic nail connection tests. Can. J. Civil 1992; 19 (1): 97-104.

[20] Pacific Earthquake Engineering Research Center (PEER). PEER strong motion database.<http://peer.berkeley.edu/smcat/>. [accessed 18.10.09].

[21] Henry RS, Sritharan S, Ingham JM. Recentering requirements for the seismic design of self-centering systems. Auckland, New Zealand: Proc of ninth Pacific Conference on Earthquake Engineering; 2011.